

# Low Raman-noise correlated photon-pair generation in a dispersion-engineered chalcogenide $\text{As}_2\text{S}_3$ planar waveguide

Matthew J. Collins,<sup>1</sup> Alex S. Clark,<sup>1</sup> Jiakun He,<sup>1</sup> Duk-Yong Choi,<sup>2</sup> Robert J. Williams,<sup>3</sup> Alexander C. Judge,<sup>1</sup> Steve J. Madden,<sup>2</sup> Michael J. Withford,<sup>3</sup> M. J. Steel,<sup>3</sup> Barry Luther-Davies,<sup>2</sup> Chunle Xiong,<sup>1,\*</sup> and Benjamin J. Eggleton<sup>1</sup>

<sup>1</sup>Centre for Ultrahigh bandwidth Devices for Optical Systems (CUDOS), Institute of Photonics and Optical Science (IPOS), School of Physics, University of Sydney, NSW 2006, Australia

<sup>2</sup>CUDOS, Laser Physics Centre, Research School of Physics and Engineering, Australian National University, Canberra ACT 0200, Australia

<sup>3</sup>CUDOS, MQ Photonics Research Centre, Department of Physics and Astronomy, Macquarie University, NSW 2109, Australia

\*Corresponding author: chunle@physics.usyd.edu.au

Received June 5, 2012; revised July 3, 2012; accepted July 3, 2012;  
posted July 3, 2012 (Doc. ID 169919); published August 8, 2012

We demonstrate low Raman-noise correlated photon-pair generation in a dispersion-engineered 10 mm  $\text{As}_2\text{S}_3$  chalcogenide waveguide at room temperature. We show a coincidence-to-accidental ratio (CAR) of 16.8, a 250 times increase compared with previously published results in a chalcogenide waveguide, with a corresponding brightness of  $3 \times 10^5$  pairs  $\cdot$  s<sup>-1</sup>  $\cdot$  nm<sup>-1</sup> generated at the chip. Dispersion engineering of our waveguide enables photon passbands to be placed in the low spontaneous Raman scattering (SpRS) window at 7.4 THz detuning from the pump. This Letter shows the potential for  $\text{As}_2\text{S}_3$  chalcogenide to be used for nonlinear quantum photonic devices. © 2012 Optical Society of America

OCIS codes: 130.4310, 190.5650, 270.0270.

Integrated devices fabricated using highly nonlinear materials are attractive for applications in quantum communication [1] including the generation of correlated photon pairs at telecommunication wavelengths and quantum frequency conversion of single photons [2]. Currently, the most commonly used integrated platforms are periodically poled  $\chi^{(2)}$  waveguides [3,4], which require accurate temperature control to achieve quasi-phase matching, and silicon-on-insulator  $\chi^{(3)}$  devices [5], whose high power performance is affected by two-photon absorption and the formation of free carriers. An alternate platform is  $\text{As}_2\text{S}_3$  chalcogenide glass, which has a high nonlinearity, low two-photon absorption, and no free carriers in addition to photosensitive properties that can be exploited for on-chip filtering [6].  $\text{As}_2\text{S}_3$  glass has been used in photonics for decades, successfully applied to ultrafast signal processing [7], sensing [8], and, recently, quantum optics in the form of correlated photon-pair generation in  $\text{As}_2\text{S}_3$  planar waveguides by spontaneous four-wave mixing (SFWM). However, a limit in the performance of  $\text{As}_2\text{S}_3$  photon-pair sources has been observed due to spontaneous Raman scattering (SpRS) [9]. In silica, which like  $\text{As}_2\text{S}_3$  chalcogenide is an amorphous glass, the detrimental effect of SpRS has also been observed and is shown to be partially mitigated by cooling to cryogenic temperatures [10–12]. This is impractical for deployment in real quantum networks; therefore an alternative solution is required to exploit the advantageous properties of  $\text{As}_2\text{S}_3$  for quantum photonics.

In this Letter we report a dramatic improvement to the correlated photon-pair statistics over those previously achieved using an  $\text{As}_2\text{S}_3$  glass chip device [9], with a room temperature coincidence-to-accidental ratio (CAR) of 16.8, more than two orders of magnitude enhancement and now at a level useful for quantum communications. Building upon our initial theoretical work [13], this result

was made possible by careful dispersion-engineering for broadband SFWM, allowing the photon passbands to be placed in the low Raman window, 7.4 THz detuned from the pump [14].

Our device, illustrated in the Fig. 1 inset, is a 10 mm long rib waveguide, 2  $\mu\text{m}$  wide and 350 nm high above a 500 nm  $\text{As}_2\text{S}_3$  layer, deposited on a silica-on-silicon substrate and overlaid with a polymer layer. The propagation loss is 0.3 and 0.8 dB  $\cdot$  cm<sup>-1</sup> in the TE and TM modes, respectively, with 5.0 dB per facet insertion loss. The nonlinear coefficient  $\gamma$  was measured to be 10 W<sup>-1</sup> m<sup>-1</sup>, and the dispersion parameter  $D$  calculated at the pump wavelength of 1545.4 nm is  $-209$  ps  $\cdot$  nm<sup>-1</sup> km<sup>-1</sup> and 25.5 ps  $\cdot$  nm<sup>-1</sup> km<sup>-1</sup> for the TE and TM modes. In our previous work, the propagation loss of the longer waveguide restricted us to TE operation, limiting the SFWM bandwidth to the region  $\pm 1.4$  THz about the pump where the SpRS efficiency is high [9].

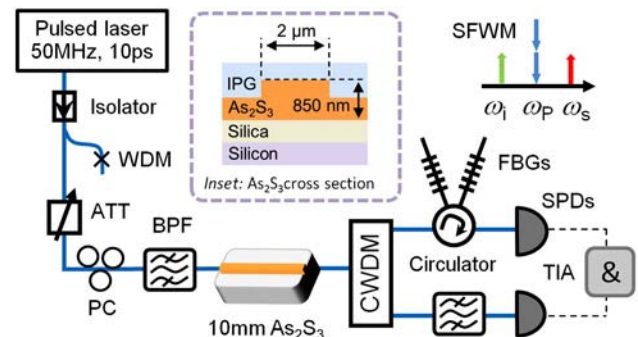


Fig. 1. (Color online) Experimental setup for correlated photon-pair generation via SFWM. ATT, attenuator; PC, polarization controller; SPD, single-photon detector; TIA, time interval analyzer; remaining acronyms defined in text. Inset: cross section of  $\text{As}_2\text{S}_3$  waveguide. IPG, inorganic polymer glass.

The key here is the tailoring of the dispersion of the waveguide and the use of a shorter device, enabling TM mode operation and SFWM up to a bandwidth of more than 9 THz. The TE and TM SFWM pair generation rate,

$$R_{\text{SFWM}} = \Delta\nu\sigma(\gamma P_0 L)^2 \text{sinc}^2\left(\frac{\beta_2(2\pi\nu)^2}{2}L + \gamma P_0 L\right), \quad (1)$$

is shown in Fig. 2, where the characteristic filter bandwidth is  $\Delta\nu$ , duty cycle  $\sigma$ , detuning from the pump  $\nu$ , the device length  $L$ , and the peak pump power  $P_0$ . The approximate SpRS photon generation rate [14],

$$R_{\text{SpRS}} = C_{\text{coupling}}\Delta\nu\sigma P_0 L g(\nu)[1 + n(\nu, T)]\frac{1}{\nu}, \quad (2)$$

is also shown in Fig. 2 and includes a coupling coefficient  $C_{\text{coupling}}$ , the phonon density of states  $g(\nu)$ , temperature  $T$ , and the boson occupation statistics

$$n(\nu, T) = \frac{1}{e^{\frac{h\nu}{k_B T}} - 1}. \quad (3)$$

The minimum in the SpRS spectrum results from a characteristic dip in the optical phonon density of states for amorphous  $\text{As}_2\text{S}_3$  glass. This low Raman window, together with the broadband SFWM enabled by the dispersion engineering, allows the efficient generation of low-noise correlated photon pairs in the TM mode [13], shown in the shaded region of Fig. 2.

Figure 1 shows our experimental setup. A mode-locked tunable fiber laser (Pritel) produced 10 ps pulses at a repetition rate of 50 MHz. These passed through an isolator, followed by a 1550/980 nm wavelength division multiplexer (WDM) to block any residual cavity pump photons. An attenuator and a polarization controller conditioned the pulses before reaching a bandpass filter (BPF) centered at 1545.4 nm, positioned directly before the chip to block any SpRS photons generated in the preceding silica fibers. The pump pulses were then coupled into the waveguide using a lensed fiber. In the far detuned case, a coarse WDM separated the signal

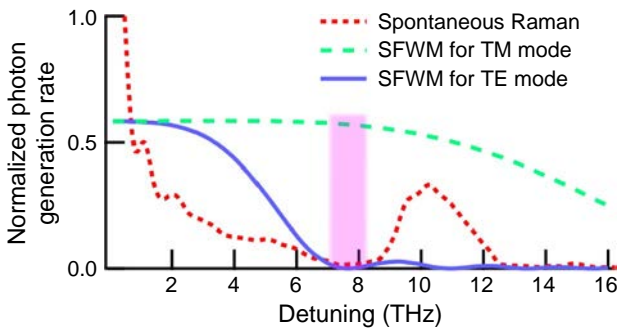


Fig. 2. (Color online) Calculation of the normalized photon generation rates versus detuning from the pump for  $\gamma P_0 L = 0.1$ . The short dashed line shows the SpRS rate [14], with a characteristic minimum at 7.4 THz (shaded). The long dashed and solid lines are the SFWM correlated pair generation for TM and TE modes, respectively. Pair generation extends to the low Raman window only for the TM mode [13].

and idler, providing 50 dB of pump suppression. A four-port circulator with two narrow-band apodized point-by-point fiber Bragg gratings (FBG) with a 0.3 nm bandwidth [15] filtered the signal photons at 1489.4 nm, while a tunable BPF with 0.5 nm bandwidth was used for the idler photons at 1605.7 nm, together providing an additional 50 dB of out-of-band noise suppression. Photons were detected by InGaAs single-photon detectors (ID210) triggered at 50 MHz with a 1 ns detection window synchronous with the pump laser. The dead time was set to 10  $\mu\text{s}$ , and the detector dark count rates were  $\approx 120 \text{ s}^{-1}$  and  $200 \text{ s}^{-1}$  for the signal and idler, respectively. In the near detuned case, a low-loss arrayed waveguide grating (AWG) was used to separate the idler and signal with 0.5 nm channel bandwidth, followed by two C-band BPFs. Taking into account the component losses and detector quantum efficiencies, we estimate the total collection efficiency for each channel at 0.2% and 0.13% for the near and far detuned cases, respectively.

We define the CAR as the ratio of the rate of correlated event counts  $C$  to the rate of noise counts  $A$ . A high CAR is desirable, indicating a better signal-to-noise ratio. A coincidence event occurs when two photons are detected with timing correlated to the same pump pulse, plotted in Fig. 3 as triangles. Detection events separated by an additional pump period are accidentals, shown in Fig. 3 as squares, and include detector dark counts, pump leakage, multiple-pair generation, and SpRS noise photons. The true coincidence rate  $C$  is the rate of detection for photon pairs generated by SFWM and given by  $C = C_{\text{raw}} - A$ , where  $C_{\text{raw}}$  is the total detected coincidence rate. In Fig. 3(a),  $A$  is small and  $C$  approaches  $C_{\text{raw}}$ , as SFWM is dominant in the low Raman window. In contrast, in Fig. 3(b),  $A$  is comparable to  $C$ , as SpRS introduces uncorrelated noise when operating close to the pump.

We measured the CAR as a function of pump power to determine the lowest noise operating point. The signal and idler channels were positioned in the low Raman window at 7.4 THz either side of the pump, enabling us to achieve a maximum CAR of 16.8, shown in Fig. 4

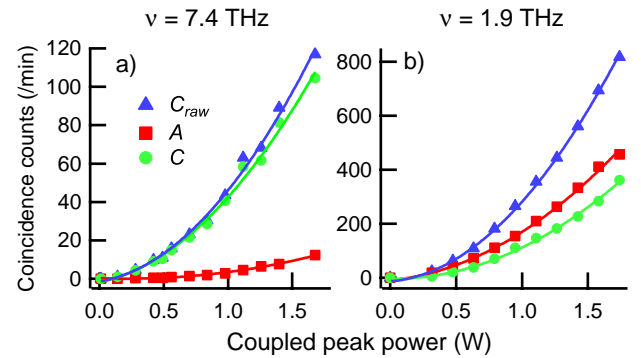


Fig. 3. (Color online) (a) Coincidence count rate versus peak power, for pairs generated in the low Raman window at  $\nu = 7.4$  THz. Here, the true coincidence count rate  $C$  approaches the total coincidence rate  $C_{\text{raw}}$ , as SFWM is dominant over noise  $A$ . (b) For small detuning  $\nu = 1.9$  THz,  $C$  and  $A$  are comparable, as SpRS is significantly more efficient at this detuning. Poissonian error bars are equal to the size of plot markers.

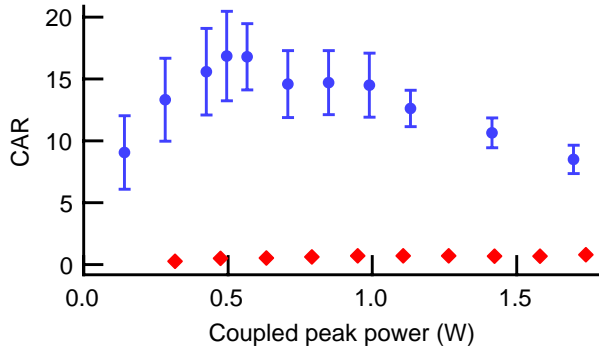


Fig. 4. (Color online) Measured CAR: for small detuning (red diamonds) and operating in the low Raman window (blue circles) with Poissonian errors bars included.

as circles, corresponding to a coupled peak power of 0.5 W, 0.002 pairs per pump pulse and nonlinear phase shift  $\gamma P_0 L = 0.05$ . The brightness at the chip was  $3 \times 10^5$  pairs  $\cdot$  s $^{-1}$   $\cdot$  nm $^{-1}$ , inferred from the detected coincidence rate and the collection efficiency. Further improvement to the CAR was limited due to loss and poor detection efficiency at the longer wavelength. Shifting the passbands to 1.9 THz from the pump we measured a maximum CAR of 0.7, shown in Fig. 4 as diamonds.

It should be noted that the CAR of 0.7 measured for small detuning is still an order of magnitude improvement from the previous CAR of 0.07 measured in a CW experiment at similar detuning [9]. This was due to the use of a pulsed pump laser enabling us to gate the detectors in synchrony with the arrival of the generated photons and access higher peak powers. The additional 25 times improvement is due to the dispersion engineering allowing access to the low Raman window.

To measure the second-order correlation function  $g^{(2)}(0)$  [16], we included a 50/50 coupler in the idler channel and replaced the single ID210 detector with a pair of ID201 detectors at the coupler outputs. The efficiency of the signal detector was increased to the maximum available (25% quoted at 1550 nm), corresponding to a heralding rate of 6.5 kHz. The higher detection efficiency improved the rate of threefold coincidences required to measure  $g^{(2)}(0)$  for a heralded source. This also dramatically increased the dark count rate to 3.5 kHz, limiting the minimum value of  $g^{(2)}(0)$ . For a coupled peak power of 0.84 W, we measured  $g^{(2)}(0) = 0.25 \pm 0.13$ . This is well below the criterion of  $g^{(2)}(0) = 0.5$  required to demonstrate single-photon antibunching. This confirmed our source was operating in the quantum regime and that it can be used as a heralded single-photon source.

In conclusion, low Raman-noise correlated photon pairs were generated in the low Raman window using a 10 mm long dispersion-engineered As $_2$ S $_3$  planar waveguide.

A CAR of 16.8 was measured at room temperature using a pulsed pump—a 250 times improvement over the original near detuned CW pumped experiment. This Letter shows the potential for As $_2$ S $_3$  waveguides to be used as a platform for quantum photonics and communications. These results not only apply to the generation of correlated photon pairs, but also to photonic manipulation through the use of As $_2$ S $_3$  glass to perform quantum state translation [2] and coherent photon conversion [17], where the single-photon and pump channels must be carefully placed to avoid contamination by SpRS.

This work was supported by the Centre of Excellence, Federation Fellowship, and Discovery Early Career Researcher Award (DECRA) programs of the Australian Research Council (ARC). The Centre for Ultrahigh bandwidth Devices for Optical Systems (CUDOS) is an ARC Centre of Excellence (project number CE110001018).

## References

1. N. Gisin and R. Thew, *Nat. Photon.* **1**, 165 (2007).
2. H. McGuinness, M. Raymer, C. McKinstrie, and S. Radic, *Phys. Rev. Lett.* **105**, 093604 (2010).
3. J. Chen, A. J. Pearlman, A. Ling, J. Fan, and A. Migdall, *Opt. Express* **17**, 6727 (2009).
4. M. Hunault, H. Takesue, O. Tadanaga, Y. Nishida, and M. Asobe, *Opt. Lett.* **35**, 1239 (2010).
5. J. E. Sharping, K. F. Lee, M. A. Foster, A. C. Turner, B. S. Schmidt, M. Lipson, A. L. Gaeta, and P. Kumar, *Opt. Express* **14**, 12388 (2006).
6. B. J. Eggleton, B. Luther-Davies, and K. Richardson, *Nat. Photon.* **5**, 141 (2011).
7. M. Pelusi, F. Luan, T. D. Vo, M. R. E. Lamont, S. J. Madden, D. A. Bulla, D.-Y. Choi, B. Luther-Davies, and B. J. Eggleton, *Nat. Photon.* **3**, 139 (2009).
8. J. Heo, M. Rodrigues, S. J. Saggese, and G. H. Sigel, *Appl. Opt.* **30**, 3944 (1991).
9. C. Xiong, G. D. Marshall, A. Peruzzo, M. Lobino, A. S. Clark, D.-Y. Choi, S. J. Madden, C. M. Natarajan, M. G. Tanner, R. H. Hadfield, S. N. Dorenbos, T. Zijlstra, V. Zwiller, M. Thompson, J. G. Rarity, M. J. Steel, B. Luther-Davies, B. H. Eggleton, and J. L. O'Brien, *Appl. Phys. Lett.* **98**, 051101 (2011).
10. X. Li, J. Chen, P. Voss, J. Sharping, and P. Kumar, *Opt. Express* **12**, 3737 (2004).
11. H. Takesue and K. Inoue, *Opt. Express* **13**, 7832 (2005).
12. S. D. Dyer, M. J. Stevens, B. Baek, and S. W. Nam, *Opt. Express* **16**, 9966 (2008).
13. C. Xiong, L. G. Helt, A. C. Judge, G. D. Marshall, M. J. Steel, J. E. Sipe, and B. J. Eggleton, *Opt. Express* **18**, 16206 (2010).
14. R. J. Kobliska and S. A. Solin, *Phys. Rev. B* **8**, 756 (1973).
15. R. J. Williams, C. Voigtländer, G. D. Marshall, A. Tünnermann, S. Nolte, M. J. Steel, and M. J. Withford, *Opt. Lett.* **36**, 2988 (2011).
16. R. Hanbury Brown and R. Q. Twiss, *Nature* **177**, 27 (1956).
17. N. K. Langford, S. Ramelow, R. Prevedel, W. J. Munro, G. J. Milburn, and A. Zeilinger, *Nature* **478**, 360 (2011).



## Optics Letters

[◀ BACK TO RESULTS](#)**JCR®Web**

Click highlighted text for a new search on that item.

Table of Contents: [Click here to view](#)

ISSN: 0146-9592

Title: Optics Letters [▼ Additional Title Information](#)

Publishing Body: Optical Society of America

Country: United States

Status: Active

Start Year: 1977

Frequency: Semi-monthly

Volume Ends: Jan - Dec

Document Type: Journal; Academic/Scholarly

Refereed: Yes

Abstracted/Indexed: Yes

Media: Print

Alternate Edition ISSN: [1539-4794](#)

Size: Standard

Language: Text in English

Price: USD 2,650 combined subscription per year domestic to institutions (Print &amp; Online Eds.)

USD 2,735 combined subscription per year in Canada to institutions (Print &amp; Online Eds.)

USD 2,840 combined subscription per year elsewhere to institutions (Print &amp; Online Eds.)

(effective 2010)

Subject: [PHYSICS - OPTICS](#)

Dewey #: 535

LC#: QC350

CODEN: OPLEDP

Special Features: Illustrations

Article Index: Index Available

Composition: Web, offset

Editor(s): Alan E Willner (Editor-in-Chief)

URL: <http://www.opticsinfobase.org/ol/journal/ol/about.cfm>

Description: Covers the latest research in optical science, including atmospheric optics, quantum electronics, fourier optics, integrated optics, and fiber optics.

### ADDITIONAL TITLE INFORMATION

Alternate Title: Medline Abbreviated title: Opt Lett; Abbreviated title: O L

[▲ Back to Top](#)

Add this item to:

**+** **ADD****Request this title:**I'd like to request this title. **GO****Corrections:**Submit corrections to Ulrich's about this title. **GO****Publisher of this title?**If yes, click GO! to contact Ulrich's about updating your title listings in the Ulrich's database. **GO**[Print](#) • [Download](#) • [E-mail](#)[▲ Back to Top](#)